Supporting Information

Wright et al. 10.1073/pnas.1501698112

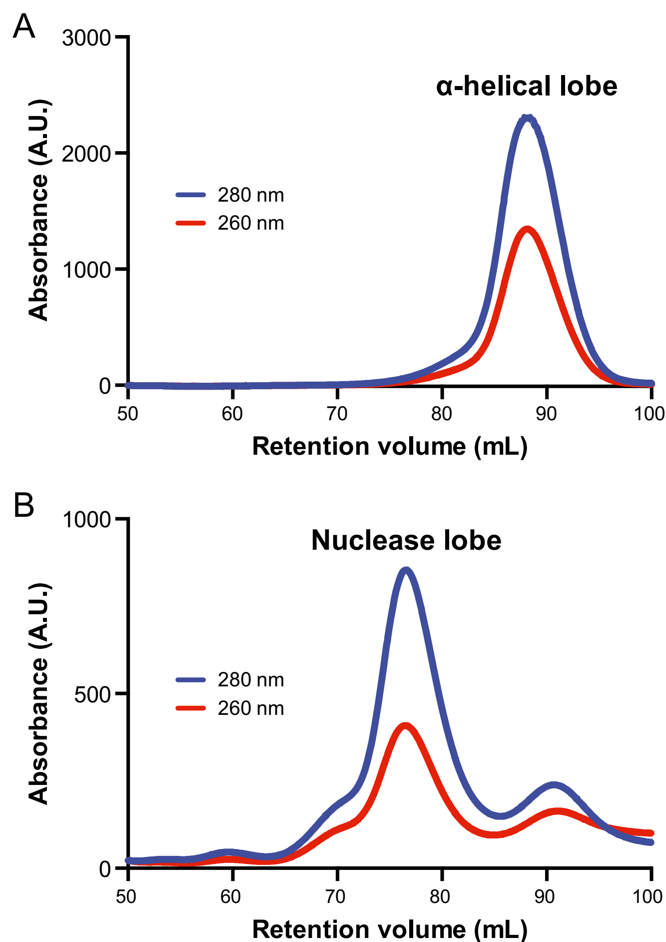

Fig. S1. Size-exclusion chromatograms of purified α-helical (*A*) and nuclease (*B*) lobes. After cleavage of the affinity tag by TEV protease and further clean-up using ortho-Ni-NTA and ion-exchange columns (α-helical lobe) or an ortho-Ni-NTA column alone (nuclease lobe), the polypeptides were concentrated and injected onto a HiLoad 16/60 Superdex 200 gel filtration column. The α-helical (77 kDa) and nuclease lobes (81 kDa) eluted at 88.4 mL and 76.8 mL, respectively. Both polypeptides were soluble and exhibited consistent activity across multiple rounds of freeze–thawing.

Fig. S2. Split-Cas9 activity is mediated by single-guide and dual-guide RNAs and requires RNA:DNA complementarity and a PAM. (*A*) DNA cleavage time courses using a single-guide RNA and WT Cas9, individual α-helical and nuclease lobes, or split-Cas9. Values for WT and split-Cas9 were averaged from three independent experiments, and error bars represent the SD. Rate constants can be found in Table S1. (*B*) DNA cleavage time courses using a dual-guide RNA (crRNA:tracrRNA hybrid) and WT Cas9 or split-Cas9. Data are presented as in *A*. (*C*) DNA cleavage assay with split-Cas9 and DNA substrates containing a mismatched target or mutated PAM (Table S2), analyzed by denaturing PAGE. Reactions contained ∼1 nM radiolabeled dsDNA and 100 nM Cas9–sgRNA complex.

Fig. S3. Split-Cas9 exhibits substantially weaker binding affinity for target DNA than WT Cas9. (*A*) Radiolabeled target dsDNA was incubated with increasing concentrations of Cas9–sgRNA complexes using catalytically inactive mutants of WT Cas9 and the nuclease lobe, and reaction products were resolved by native PAGE. The distinct Cas9 constructs in each titration are indicated at the top. (*B*) Quantified binding data from *A*. Split dCas9–RNA binds dsDNA with an apparent equilibrium dissociation constant of ∼700 nM, which is more than three orders of magnitude greater than that determined for dCas9–RNA (K_d ∼0.2 nM). However, the apparent affinity measured here is likely to be much weaker than the actual affinity because the low split dCas9–sgRNA concentrations that were tested will also favor dissociation of the ternary complex formed between the sgRNA, α-helical lobe, and nuclease lobe. Thus, the observed binding curve is likely a convolution of equilibria between the protein and sgRNA, and between the protein–sgRNA complex and dsDNA. Individual lobes together with sgRNA do not appreciably bind dsDNA at the tested concentrations.

Fig. S4. Split-Cas9 heterodimerization requires the sgRNA. (*A–D*) Raw electron micrographs of negatively stained α-helical and nuclease lobes alone (*A* and *B*), together (*C*), or together with sgRNA (*D*). Particles having dimensions consistent with WT Cas9–RNA complexes, and thus indicative of heterodimer formation, are observed only in the presence of sgRNA. Representative particles are circled (yellow). (Scale bars: 50 nm.)

Fig. S5. Excess sgRNA reduces the DNA cleavage activity of split-Cas9. DNA cleavage assay with varying molar ratios of protein to sgRNA, analyzed by denaturing PAGE. Reactions contained ∼1 nM radiolabeled dsDNA, 100 nM α-helical and nuclease lobes, and 50–1,000 nM sgRNA. The extent of product formation decreases substantially as the sgRNA concentration surpasses the lobe concentration. This observation suggests that stoichiometric excesses of sgRNA titrate the individual lobes away from each other and onto independent sgRNA molecules, a hypothesis supported by the finding that distinct sgRNA motifs interact with either lobe.

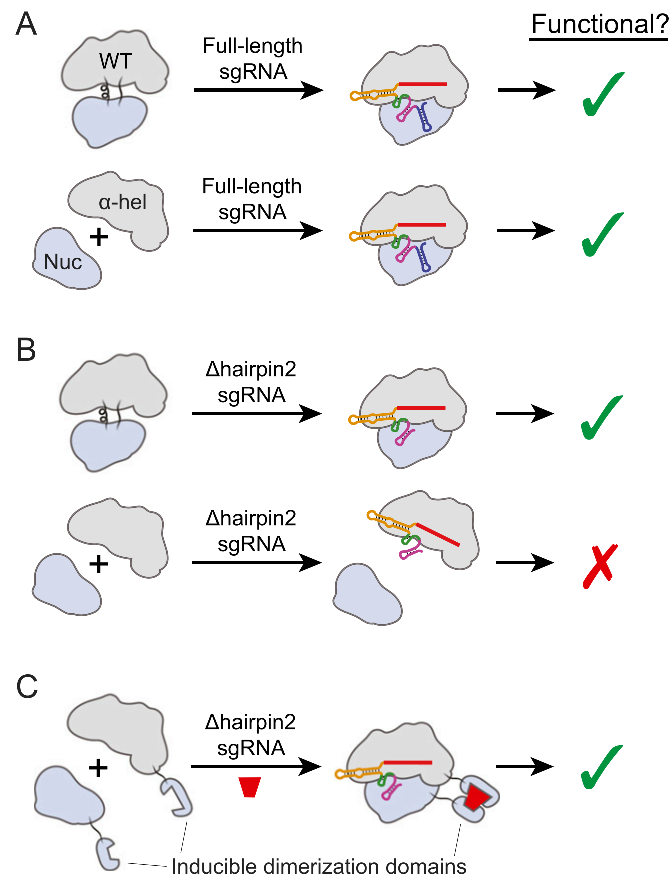

Fig. S6. Strategy for inducible control of genome engineering by a split-Cas9 enzyme complex. (*A*) Because the α-helical and nuclease lobes dimerize in the presence of sgRNA, both WT and split-Cas9 are functional genome editing tools in cells using full-length sgRNA. (*B*) sgRNA variants with 3′-hairpin truncations have substantially weaker affinity for the nuclease lobe and thus do not efficiently assemble a functional split-Cas9 complex, leading to an inactive enzyme. In contrast, in vitro DNA cleavage by WT Cas9 is minimally affected by these truncations, indicating that the intrinsic activity of the Cas9–sgRNA enzyme complex does not require hairpins at the 3′ end. (*C*) We propose an inducible split-Cas9 system, in which exogenous dimerization domains control the assembly of a functional ternary complex between a 3′-truncated sgRNA and the α-helical and nuclease lobes. By fusing both lobes to domains that dimerize only upon some external stimulus (e.g., a small molecule; red trapezoid), split-Cas9 can be specifically activated for a desired genome-engineering outcome.

Fig. S7. The 3′-truncated sgRNA variants selectively inactivate split-Cas9. (*A* and *B*) DNA cleavage assays with WT and split-Cas9 and a panel of four different sgRNAs, analyzed by denaturing PAGE. (*A*) Full-length sgRNAs promote DNA cleavage activity of both WT and split-Cas9 whereas split-Cas9 activity is completely lost with an sgRNA lacking both hairpins at the 3′ end (Δhairpins1-2). (*B*) sgRNA variants where only one hairpin is removed show minimal effects on WT Cas9 activity but severely (Δhairpin2) or completely (Δhairpin1) inactivate split-Cas9.

Table S1. Cleavage rate constants for WT and split-Cas9 using different sgRNA constructs

	Rate constant (k_{obs}) for indicated sgRNA*, min^{-1}		
Protein	Full-length	ΔHairpin1	ΔHairpins1-2
WT Cas9	11.3 ± 0.9	9.2 ± 0.4	6.0 ± 0.6
α-Helical lobe	N.D.	—	—
Nuclease lobe	N.D.	—	—
Split-Cas9	1.0 ± 0.2	$(5.5 \pm 0.8) \times 10^{-4}$	N.D.

N.D., cleavage not detected; —, experiment not performed.
*Three independent experiments were performed for each condition, and the values represent the mean ± SEM.

Table S2. DNA and RNA substrates used in this study

Description	Sequence*	Used in Figs.
λ1 target dsDNA	5′-AGCAGAAATCTCTGCTGACGCATAAAGATGAGACGCTGGAGTACAAACGTCAGCT-3′ 3′-TCGTCTTTAGAGACGACTGCGTATTTCTACTCTGCGACCTCATGTTTGCAGTCGA-5′	1D, 3C, S2A, S2B, S3, S5, S7
λ1 target dsDNA, mutated PAM	5′-AGCAGAAATCTCTGCTGACGCATAAAGATGAGACGCTCGAGTACAAACGTCAGCT-3′ 3′-TCGTCTTTAGAGACGACTGCGTATTTCTACTCTGCGAGCTCATGTTTGCAGTCGA-5′	S2C
λ2 target dsDNA, (λ1 mismatch)	5′-GAGTGGAAGGATGCCAGTGATAAGTGGAATGCCATGTGGGCTGTCAAAATTGAGC-3′ 3′-CTCACCTTCCTACGGTCACTATTCACCTTACGGTACACCCGACAGTTTTAACTCG-5′	S2C
λ1 sgRNA, full-length	5′-GACGCAUAAAGAUGAGACGCGUUUUAGAGCUAUGCUGUUUUGGAAACAAAACAGCAU- AGCAAGUUAAAAUAAGGCUAGUCCGUUAUCAACUUGAAAAAGUGGCACCGAGUCGGUG- CUUUUUUUGGAUC-3′	1D, 2C, 2E, 3C, S2A, S2C, S3, S4D, S5, S7A
λ1 crRNA	5′-GACGCAUAAAGAUGAGACGCGUUUUAGAGCUAUGCUGUUUUG-3′	2E, S2B
TracrRNA	5′-GGACAGCAUAGCAAGUUAAAAUAAGGCUAGUCCGUUAUCAACUUGAAAAAGUGGCAC- CGAGUCGGUGCUUUUU-3′	2E, S2B
λ1 sgRNA, Δhairpin1 and -2	5′-GACGCAUAAAGAUGAGACGCGUUUUAGAGCUAUGCUGUUUUGGAAACAAAACAGCAU- AGCAAGUUAAAAUAAGGCUAGUCCGUGGAUC-3′	2D, 3C, S7A
λ1 sgRNA, Δhairpin2	5′-GACGCAUAAAGAUGAGACGCGUUUUAGAGCUAUGCUGUUUUGGAAACAAAACAGCAU- AGCAAGUUAAAAUAAGGCUAGUCCGUUAUCAACUUGAAAAAGUGGAUC-3′	S7B
λ1 sgRNA, Δhairpin1	5′-GACGCAUAAAGAUGAGACGCGUUUUAGAGCUAUGCUGUUUUGGAAACAAAACAGCAU- AGCAAGUUAAAAUAAGGCUAGUCCGUUGGCACCGAGUCGGUGCUUUUUUU-3′	S7B
λ1 sgRNA, Δspacer–nexus	5′-GGUAUCAACUUGAAAAAGUGGCACCGAGUCGGUGCUUUUUUU-3′	2D
EMX1 sgRNA, full-length	5′-GGUCACCUCCAAUGACUAGGGGUUUAAGAGCUAUGCUGGAAACAGCAUAGCAAGUUU- AAAUAAGGCUAGUCCGUUAUCAACUUGAAAAAGUGGCACCGAGUCGGUGCUUUUUU-3′	3B

*RNA guide sequences and complementary DNA target strand sequences are shown in red; PAM sites are highlighted in yellow.